THE ASTROPHYSICAL JOURNAL, 394:L37–L41, 1992 August 1

EVIDENCE FOR SHOCK-HEATED GAS IN THE HOPKINS ULTRAVIOLET TELESCOPE SPECTRUM OF NGC 1068

GERARD A. KRISS,[1] ARTHUR F. DAVIDSEN,[1] WILLIAM P. BLAIR,[1]
HENRY C. FERGUSON,[2] AND KNOX S. LONG[1,3]
Received 1992 April 6; accepted 1992 May 12

ABSTRACT

We obtained far-UV spectra of the prototypical Seyfert 2 galaxy NGC 1068 with the Hopkins Ultraviolet Telescope during the flight of Astro-1 aboard the space shuttle Columbia in 1990 December. In two separate observations of NGC 1068 lasting 2356 and 2692 s we used circular apertures of 18″ and 30″ diameter, respectively. The spectra reveal strong emission lines of C III λ977, N III λ991, Lyβ, O VI λλ1032, 1038, and He II λ1085, all seen for the first time in a Seyfert 2 galaxy. Longward of Lyα the spectrum is similar to previous observations obtained with the *IUE*. Broad-line components are visible for both Lyα and C IV. The relative ratios of broad Lyα, C IV, and Hβ are typical of those seen in Seyfert 1 galaxies and QSOs. A flat, blue continuum is observed down to the Lyman limit imposed by interstellar absorption in our own Galaxy. Excess continuum emission is present through the 30″ aperture which can plausibly be attributed to young stars in the starburst ring. The moderately strong C III λ977 and N III λ991 emission is unusual for an AGN, and the line ratios below Lyα are similar to those seen in HUT observations of the Cygnus Loop supernova remnant. The ratios of C III] λ1909 to λ977 and N III] λ1750 to λ991 imply temperatures exceeding 26,700 K and 24,000 K, respectively. Since these temperatures are much higher than those typically encountered in photoionized gas with abundant C^{+2} and N^{+2} populations, shock heating should be reconsidered as an additional source of emission lines in the nucleus of NGC 1068. Shocks could arise from the interaction of an X-ray–heated wind from the nucleus with the surrounding interstellar medium, or from radio jets striking interstellar clouds. Shocks from supernovae in starburst regions near the active nucleus are not a likely explanation.

Subject headings: galaxies: individual (NGC 1068) — galaxies: nuclei — galaxies: Seyfert — ultraviolet: general

1. INTRODUCTION

The active galaxy NGC 1068 is the nearest and brightest of the Seyfert galaxies, and it is the prototype of the Seyfert 2 class. Lawrence & Elvis (1982) have suggested that Seyfert 1 and 2 galaxies are similar phenomena related by varying degrees of obscuration and orientation. The discovery of *polarized* emission from broad permitted lines with widths of a few thousand km s^{-1}, the defining characteristic of Seyfert 1 galaxies, by Antonucci & Miller (1985) provides a more concrete realization of this hypothesis—the nuclear continuum and broad-line region are obscured from direct view by an opaque, molecular torus, and a hot electron plasma scatters the radiation into our line of sight.

The nuclear region of NGC 1068 hosts a wide variety of astrophysical phenomena. An ellipse of H II regions, starburst knots, and CO emission at an average radius of 18″ encircles the nucleus and the narrow-line region. Interior to this, the conical shape of the emission-line clouds in the extended narrow-line region suggests either an anisotropic radiation field or collimated outflow from the nuclear region (Pogge 1988; Evans et al. 1991). Many of the bright [O III] clouds observed by Evans et al. (1991) coincide with knots of radio emission. Krolik & Begelman (1986) modeled the electron scattering region as an X-ray–heated wind and predicted strong fluorescent Fe emission which was subsequently detected in X-ray observations (Elvis & Lawrence 1988; Koyama et al. 1989; Marshall 1991). With the additional diagnostic emission lines at wavelengths shortward of Lyα made accessible by the far-UV sensitivity of the Hopkins Ultraviolet Telescope (HUT), our observations of NGC 1068 were planned to help unravel the complex physical conditions in the nuclear region.

2. OBSERVATIONS AND DATA REDUCTION

The 0.9 m primary mirror in HUT gathers light for a prime-focus, Rowland-circle spectrograph with a photon-counting detector (Davidsen et al. 1992). First-order spectra cover the 830–1860 Å spectral range with a point-source resolution of ~3Å. On 1990 December 8, in two separate pointings centered on the optical nucleus of NGC 1068 lasting 2356 and 2692 s, we used circular apertures of 18″ and 30″ diameter, respectively (2.0 and 3.3 kpc for a distance of 23 Mpc). In Figure 1 (Plate L5) the apertures are shown superposed on an image of NGC 1068 in the light of Hα+[N II]. The 18″ aperture covers only the narrow line region near the nucleus, but the larger aperture includes portions of the H II regions in the starburst ring. The highest quality data were obtained during orbital night when the airglow contamination is at a minimum. For the spectra obtained through the 18″ and 30″ apertures this represents total integration times of 2060 and 2162 s, respectively. The raw count rate data were corrected for pulse persistence in the phosphor readout. Detector background and grating-scattered geocoronal Lyα were determined from regions free of airglow

[1] Center for Astrophysical Sciences, Department of Physics and Astronomy, The Johns Hopkins University, Baltimore, MD 21218.
[2] Institute of Astronomy, The Observatories, Cambridge University, Madingley Road, Cambridge CB3 0HA, England, UK.
[3] Space Telescope Science Institute, 3700 San Martin Drive, Baltimore, MD 21218.

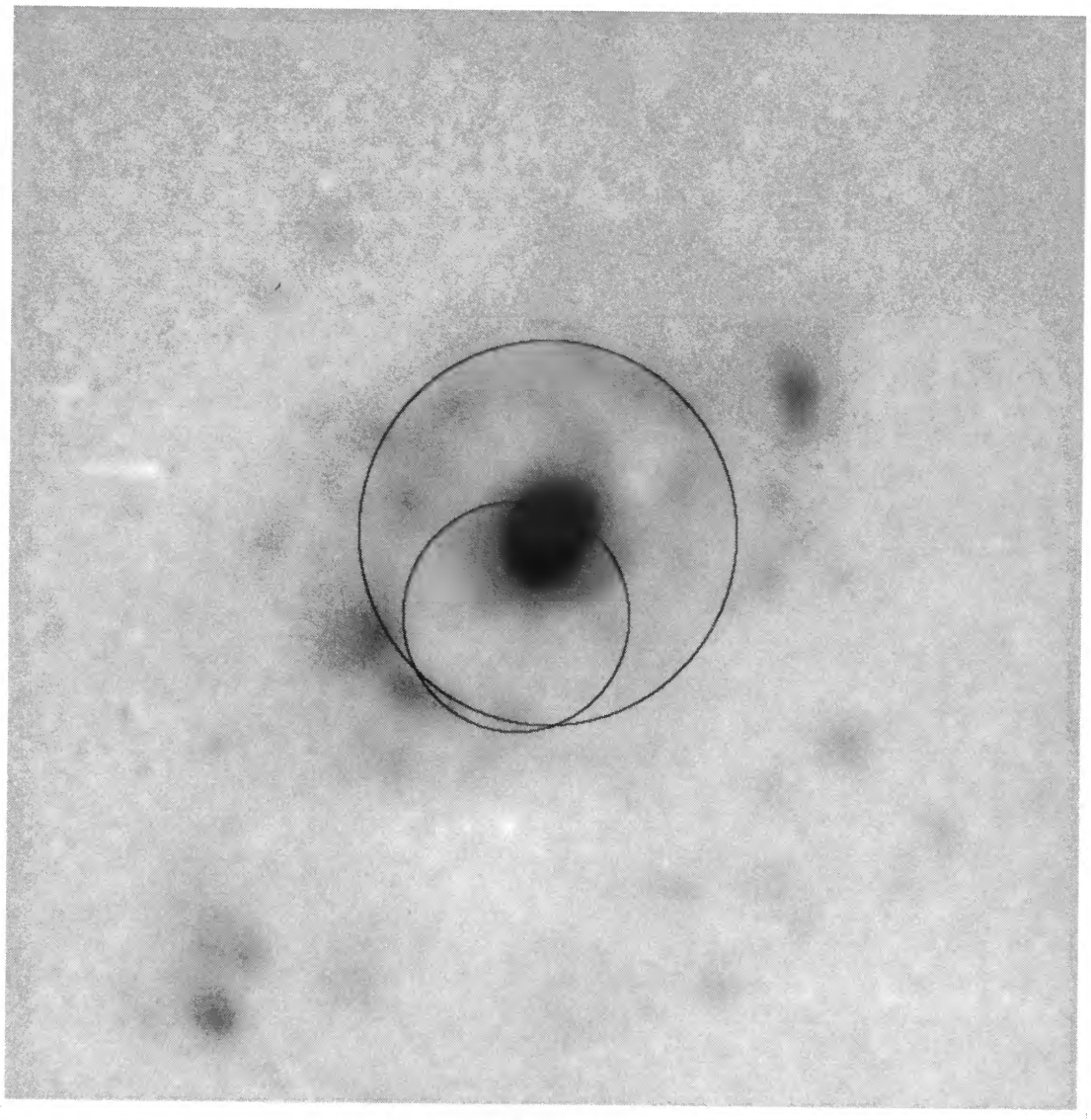

FIG. 1.—An Hα+[N II] image of the central region of NGC 1068 is shown with the relative positions of the HUT 18″ and 30″ diameter circular apertures superposed. North is up, and east is to the left. The image is a continuum-subtracted sum of six 300 s exposures through an 80 Å wide filter centered on 6606 Å obtained by H. Ford on the NOAO/KPNO No. 1 0.9 m telescope using an RCA CCD.

KRISS et al. (see 394, L37)

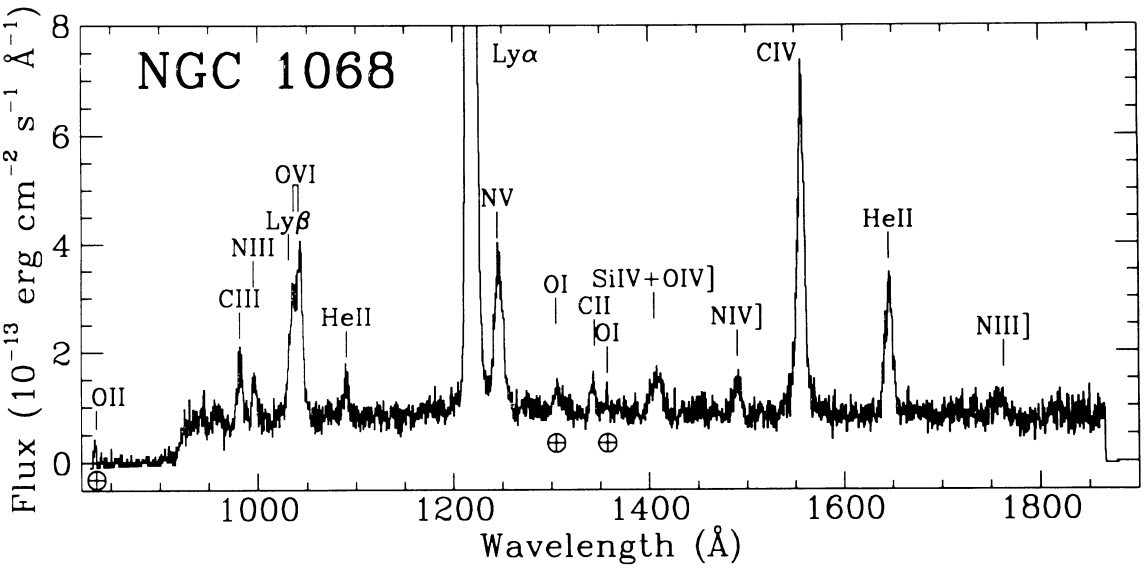

FIG. 2.—The flux-calibrated HUT spectrum of NGC 1068 as observed through the 18″ aperture. Prominent emission lines are marked, and airglow emission is indicated with an Earth symbol. Lyα from NGC 1068 is blended with geocoronal Lyα and is off scale in the figure. Of particular note in the region below Lyα are the strong emissions from C III λ977, N III λ991, Lyβ, O VI λλ1032, 1038, and He II λ1085.

below the 912 Å Lyman limit. We subtracted the background and placed the spectra on an absolute flux scale using the effective-area curve developed from preflight and postflight calibrations and on-orbit observations of the hot white dwarf G191-B2B (Davidsen et al. 1992).

Both observations were guided manually by the payload specialists with rms deviations of only 1.″8 for the first observation through the 18″ aperture and 2.″2 through the 30″ aperture. Correlating count rates with pointing errors, however, indicates that the nucleus was ~7″ from the center of the slit during the observation through the 18″ aperture. This offset combined with the measured pointing errors and an image size of ~4″ FWHM leads to a light loss of 10%–20% during the observation through the smaller aperture. This is consistent with the 1.2 Å wavelength shift observed between the two observations, and excess flux of 17% in the emission lines as measured through the 30″ aperture. (The emission-line spectrum through the 30″ aperture has exactly the same line ratios as that through the smaller aperture, a quite unexpected result if the excess line emission is coming from a physically distinct region.) We have therefore corrected the wavelengths of the 18″ aperture spectrum with a shift of 1.2 Å to longer wavelengths, and corrected the fluxes upward by 17% to account for the miscentering. With the applied wavelength shift, the observed Lyman edge matches that expected for absorption by the redshifted ISM of NGC 1068 at 1150 km s^{-1} (Meaburn & Pedlar 1986).

Figure 2 shows the flux-calibrated HUT spectrum of NGC 1068 obtained through the 18″ aperture. The spectrum obtained through the 30″ aperture is qualitatively similar, but the continuum is ~35% brighter. Since the larger aperture includes portions of the starburst ring, it is plausible that the additional light is due to young stars. The difference between the large and small aperture spectra is shown in Figure 3 binned on 10 Å intervals. The difference spectrum resembles that of a reddened early-type star, with suggestions of blue-shifted stellar absorption features at C IV λ1549, Si IV λ1396, C II λ1335, and N V λ1240. The difference spectrum is more reddened and/or of later mean spectral type than the spectrum of knot 2 in the starburst ring obtained by Hutchings et al. (1991). Without independent constraints on extinction, models with burst ages from 1–100 × 10^6 yr all fit the continuum. Young bursts such as the 5 × 10^6 yr model shown in Figure 3, however, provide a better match to the stellar absorption features.

We measure emission-line fluxes in the NGC 1068 spectrum using a nonlinear χ^2 minimization technique to fit a multicomponent model to the lines and the continuum. We assume a powerlaw in f_λ, allow for extinction according to the mean galactic curve of Seaton (1979) (assuming it is valid to 912 Å as

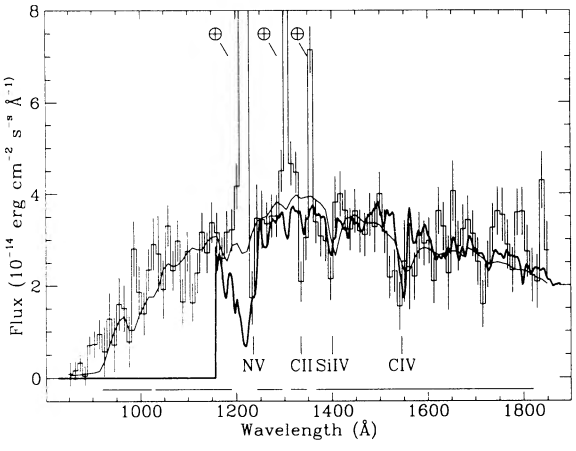

FIG. 3.—The difference of the 30″ and 18″ HUT spectra, binned in 10 Å intervals. The excess continuum in the 30″ aperture resembles a reddened early-type stellar spectrum. The smooth curve is a synthetic spectrum constructed from Kurucz (1991) modesl of a starburst viewed at an age of 5 × 10^6 yr reddened by $E_{B-V} = 0.28$. For the initial mass function we assume a Salpeter IMF (slope $x = 1.35$) with a lower mass cutoff of 0.1 $M_\odot$, and an upper mass limit of 75 $M_\odot$. The heavy solid line is constructed from a library of *IUE* stellar spectra. Wavelength intervals used in the fit are denoted by solid lines at the bottom of the figure. Residual airglow features are marked with Earth symbols. The total mass in the starburst is 0.7–2.4 × 10^8 $M_\odot$, roughly comparable to the mass of young stars in the starburst ring inferred from infrared observations (1.3–2.7 × 10^8 $M_\odot$; Thronson et al. 1989).

shown by *Voyager* observations; Longo et al. 1989), and include absorption due to neutral hydrogen both in our own Galaxy and in NGC 1068. All emission lines are well fitted by single Gaussian profiles aside from Lyα and C IV λ1549, both of which require additional broad components with FWHM ~3800 km s^{-1}. Similar broad components would not be apparent at the lower signal-to-noise ratio of the fainter emission lines. Although Lyα from NGC 1068 is blended with strong geocoronal Lyα in the HUT spectra, the redshift is high enough that we can successfully deblend the two lines using a geocoronal Lyα template developed from other blank sky night observations through the 18″ aperture. The observed emission-line fluxes, redshifts, and FWHM are listed in Table 1. The line widths have not been corrected for the instrumental resolution [~900 (1000 Å/λ) km s^{-1}]. Our observed fluxes longward of Lyα agree with the *IUE* observations of Snijders, Netzer, & Boksenberg (1986).

The low redshifts for Lyβ and O VI λ1032 and the low O VI doublet ratio of 0.77 ± 0.13 found in our deblending of the Lyβ + O VI complex suggest that there may be blueshifted absorption components associated with the O VI lines. Higher resolution spectra from the Faint Object Spectrograph on the *Hubble Space Telescope* show similar doublet ratios for N V λλ1239, 1243 and C IV λλ1548, 1551 (Armus et al. 1991).

We confirm the presence of broad emission from C IV λ1549 and Lyα reported by Snijders et al. (1986) and Armus et al. (1991). Figure 4 shows our deblending of the broad and narrow C IV emission-line components. Both C IV and Lyα have widths consistent with the FWHM of 3030 km s^{-1} measured for the broad polarized component of Hβ by Miller, Goodrich, & Mathews (1991, hereafter MGM). The redshift of broad Lyα matches that of broad Hβ, but the uncertainty in the redshift is probably larger than the purely statistical error indicated in Table 1 due to the heavy blending under geocoronal Lyα. Broad C IV λ1549, however, is blueshifted relative to narrow C IV and to the broad Hβ of MGM. Blueshifts of C IV relative to lower ionization lines such as the Balmer lines are common in the broad line regions of Seyfert 1 galaxies and quasars (Gaskell 1982; Wilkes 1984). The broad-line flux ratios of 4.9:1 for C IV to Hβ and 6.4:1 for Lyα to Hβ are also typical of Seyfert galaxies and quasars.

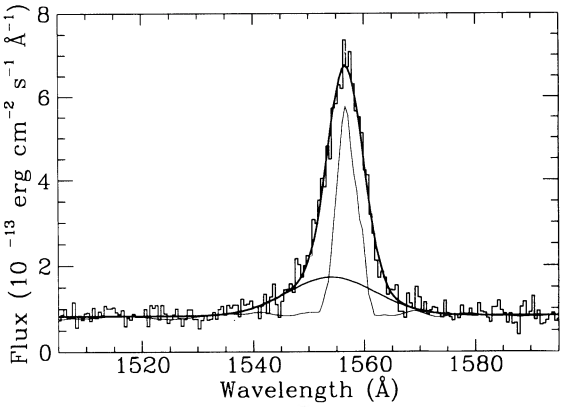

FIG. 4.—The spectral region surrounding C IV λ1549 is enlarged to illustrate the broad component of the line. The solid heavy curve is the best-fit profile composed of a narrow and a broad Gaussian. To illustrate the line spread function, the thin solid line is the C IV λ1549 profile from a HUT observation of the RS CVn star α Aur. The narrow stellar line is clearly asymmetric, but the doublet is not resolved; the stellar profile does not have the broad wings we detect in NGC 1068.

The flat continuum shape, in conjunction with the rapid increase in selective extinction below Lyα, allows us to measure the continuum reddening. For a power-law fit to our data we find $f_\lambda = 1.75 \times 10^{-13}(\lambda/1000\ \text{Å})^{-\alpha}$ ergs cm^{-2} s^{-1} Å^{-1} with $\alpha = 0.62 \pm 0.15$ and $E_{B-V} = 0.065 \pm 0.02$. Using *IUE* data, Neugebauer et al. (1980), Snijders et al. (1986), and Kinney et al. (1991) find similar power-law indices, and all have concluded that galactic-type reddening of the continuum is low based on the absence of the 2175 Å extinction feature. The He II lines λ1640 and λ1085 in our spectrum lead to a similarly low estimate for the extinction: for the observed ratio of 5.78 ± 1.62, an intrinsic ratio of 7.0 (Seaton 1978) implies $E_{B-V} = 0.05^{+0.09}_{-0.05}$.

TABLE 1

EMISSION LINES IN THE HUT SPECTRUM OF NGC 1068

Line	λ_{vac} (Å)	Flux (10^{-13} ergs cm^{-2} s^{-1})	$cz_\odot$ (km s^{-1})	FWHM (km s^{-1})
C III	977.03	7.6 ± 1.4	1436 ± 209	2091 ± 479
N III	991.00	3.9 ± 1.0	1549 ± 228	1531 ± 428
Lyβ	1025.72	12.3 ± 2.5	678 ± 203	1972 ± 0
O VI	1031.93	16.3 ± 2.2	1106 ± 156	1972 ± 0
O VI	1037.62	21.1 ± 2.2	1421 ± 111	1972 ± 245
He II	1085.15	3.7 ± 1.0	1239 ± 236	1572 ± 535
Lyα n	1215.67	101.8 ± 4.1	1543 ± 32	1442 ± 61
Lyα b	1215.67	23.8 ± 4.4	1691 ± 297	3959 ± 670
N V	1240.15	28.2 ± 1.7	1517 ± 80	2460 ± 162
C II	1334.53	3.5 ± 0.8	1705 ± 179	1300 ± 365
Si IV + O IV]	1400.00	8.8 ± 1.3	1609 ± 225	2701 ± 380
N IV]	1486.50	5.1 ± 1.1	708 ± 195	1676 ± 356
C IV n	1549.05	39.7 ± 3.0	1449 ± 55	1416 ± 110
C IV b	1549.05	18.1 ± 3.4	950 ± 314	3645 ± 795
O III] tot	1663.00	<1.5	1500 ± 0	1500 ± 0
He II	1640.50	21.4 ± 1.6	1040 ± 63	1604 ± 126
N III]	1750.00	5.7 ± 1.5	1353 ± 362	2492 ± 747

NOTES.—Error bars are ±1 σ for the appropriate number of interesting parameters as described by Avni (1976; typically 5 for an isolated emission line). Error bars set equal to zero indicate a parameter fixed at the given value.

In contrast, a variety of optical and infrared emission-line ratios consistently yield higher extinction, $E_{B-V} = 0.3$ to 0.4 (Neugebauer et al. 1980; Malkan & Oke 1983), and the ratio of 3.89 for He II λ1640 in the HUT spectrum to He II λ4686 as measured by Koski (1978) and Shields & Oke (1975) implies $E_{B-V} = 0.16$ for an assumed intrinsic ratio of 7.0 (Seaton 1978). These differences in reddening might be reconciled by adopting an extinction curve such as that observed toward θ^1 Ori C, which has a weak 2175 Å feature and a weak far-UV component (Fitzpatrick & Massa 1988). The He II λ1640 to λ1085 ratio then implies $E_{B-V} = 0.15^{+0.25}_{-0.15}$, and the ratio of λ1640 to λ4686 gives $E_{B-V} = 0.48$. Using this extinction curve for the continuum, we find $E_{B-V} = 0.11 \pm 0.03$, still substantially lower than for the emission lines. This may indicate that the obscuring material is preferentially found in or near the emission-line clouds rather than along lines of sight to the continuum-scattering region.

3. DISCUSSION

The most unusual features in our NGC 1068 spectra are the moderately strong emission lines C III λ977 and N III λ991. These emission lines have never been seen before in spectra of AGNs, including those observed with HUT during Astro-1. They are also not expected to be strong in photoionized gas because of their high excitation temperatures. However, the emission-line spectrum of NGC 1068 throughout the HUT wavelength range qualitatively resembles the HUT spectrum of a radiative shock in the Cygnus Loop supernova remnant (Blair et al. 1991b), which suggests that shock heating may contribute significantly to the line emission.

To make a more quantitative assessment of whether line excitation processes in addition to photoionization are necessary to explain the NGC 1068 emission-line spectrum, we use the C III line ratio $[I(\lambda1907) + I(\lambda1909)]/I(\lambda977)$ and the N III line ratio $I(\lambda1750)/I(\lambda991)$ as temperature diagnostics. Since the C III] $\lambda\lambda$1907, 1909 lines are outside the HUT wavelength range, we use the *IUE* measurements of Snijders et al. (1986) which give a flux of 2.4×10^{-12} ergs cm^{-2} s^{-1}. For purely collisional excitation in the low-density limit ($n_e < 10^5$ cm^{-3}) the observed C III line ratio of 3.15 ± 0.51 gives a temperature of $26{,}700^{+1900}_{-1400}$ K (90% confidence errors) using the collision strengths of Nussbaumer & Storey (1978). The N III line ratio of 1.46 ± 0.34 implies $T = 24{,}000^{+2700}_{-1800}$ K for the collision strengths of Nussbaumer & Storey (1979), or $T = 32{,}700^{+5200}_{-3200}$ K for Nussbaumer & Storey (1982). Corrections for extinction or for resonance line scattering will lead to *higher* temperatures. For $E_{B-V} = 0.4$, we deduce temperatures greater than 110,000 K. If the C III λ977 and N III λ991 emission is produced in collisionally ionized gas, such high temperatures arise naturally since both C^{+2} and N^{+2} reach their maximum relative populations in collisionally excited plasmas with $T \sim 80{,}000$ K (e.g., Shull & van Steenberg 1982).

The emission-line clouds nearest the nucleus in NGC 1068 are likely to be hot and highly ionized. Our reddening-corrected continuum implies an ionization parameter $\Xi = F_{\rm ion}/nkTc = 3.5(b/70)(10\ {\rm pc}/r)^2/n_6\ T_4$, where $F_{\rm ion}$ is the extrapolated UV powerlaw continuum integrated from 1 to 1000 Rydbergs, r is the distance of the cloud from the ionizing source ($\sim$10 pc for the nearest clouds; Evans et al. 1991), n_6 is the density in units of 10^6 cm^{-3}, T_4 is the temperature in units of 10^4 K, and b is the "boost" factor which corrects for the small percentage of the total flux actually scattered into our line of sight ($b \sim 70$; MGM). Densities within these nearest clouds must exceed $\sim 10^5$ cm^{-3} in order for them to survive (Caganoff et al. 1991). Equilibrium temperatures under these conditions are 30,000 K for typical AGN spectra (Krolik, McKee, & Tarter 1981). Although computed ratios of C III λ977 to λ1909 in photoionization calculations do match our observations, the predicted C IV λ1549 to C III] λ1909 ratios exceed 15 (Krolik 1992), much higher than the observed ratio of 1.65. Multizone models will not solve the problem—higher ionization parameters produce even more C IV emission relative to C III and eventually lead to thermal instability; lower ionization parameters reduce the C IV λ1549 flux, but the lower equilibrium temperatures result in fainter C III λ977.

As suggested by Viegas-Aldrovandi & Contini (1989), shocks may be a common feature of the narrow-line regions of AGNs. Shock models alone (e.g., Hartigan, Raymond, & Hartmann 1987) fail to account for all the observed emission lines, but, given the large region covered by our 18″ aperture, it is likely that several different emission mechanisms are required to match the whole spectrum. A simple combination of shock and photoionization models appears promising. If we normalize the model *I*160 from Hartigan et al. (1987) to the observed intensity of C III λ977, all remaining UV lines except O III] $\lambda\lambda$1661, 1667 are observed to be *brighter* than would be predicted by a 160 km s^{-1} shock; the excess emission above the shock model predictions are within ranges produced by photoionization.

For either photoionization or shock heating, the conspicuous absence of emission from O III] $\lambda\lambda$1661, 1667 in our spectrum is problematic. The high-luminosity *IRAS* galaxy 10214+4724, which resembles NGC 1068 in many respects, also has relatively weak O III] $\lambda\lambda$1661, 1667, and its spectrum bears many similarities to supernova remnants (Rowan-Robinson et al. 1991). If we apply the diagnostic ratios developed by Keenan & Aggarwal (1986) to our upper limits for $\lambda\lambda$1661, 1667 together with Koski's (1978) optical measurements of [O III] λ4363 and $\lambda\lambda$4959, 5007, we find $T < 12{,}500$ K, in contrast to the high temperatures implied by the C III and N III lines. The shock plus photoionization models of Viegas-Aldrovandi & Contini (1989) are also unable to account for the weak O III] emission. We are currently exploring alternative combinations of shocks and photoionization to develop a consistent explanation.

Shocks in NGC 1068 could be generated by supernovae in a nuclear starburst region, but we consider this to be unlikely. First, the C III and N III line emission is most prominent in our *smaller* aperture, not the aperture including portions of the known starburst ring. Second, the observed C III λ977 + N III λ991 luminosity is 1.3×10^4 times the integrated luminosity of the Cygnus Loop in the same lines (2.7×10^{36} ergs s^{-1}; Blair et al. 1991a). For a lifetime of 10^4 yr for an SNR, this implies a supernova rate of 1.2 per year. Variability on this time scale is not observed in NGC 1068. Furthermore, if the supernovae are produced by a population of B0 stars with typical lifetimes of 2×10^7 yr, 2.6×10^7 stars would be required in a steady state. The continuum emission from this stellar population would be more than 100 times what we observe in the far UV, and the blueshifted absorption features typical of early-type stars that are seen in the difference spectrum (Fig. 3) are *not* visible in the 18″ aperture spectrum.

Several other mechanisms for producing shock-heated gas in NGC 1068 are more likely. In the models of Viegas-Aldrovandi & Contini (1989), shocks form on the leading edges

of narrow-line region clouds as they circulate through a tenuous intercloud medium. In NGC 1068 the X-ray–heated wind of Krolik & Begelman (1986) could be the source of this intercloud medium. As the wind cools, it too could be a direct source of thermal emission. Finally, strong shocks could be formed as radio plasma ejected from the active nucleus collides with the narrow-line region clouds. The bright knots of [O III] emission coincident with radio bright spots (Evans et al. 1991) could be the sites of these shocks.

Without the superb efforts of the astronauts on board Columbia and of the ground crews at Marshall Space Flight Center and Johnson Space Flight Center to overcome the pointing problems on Astro-1, these observations would not have been possible. We are grateful to Holland Ford for permission to use his Hα image of NGC 1068. We also acknowledge fruitful conversations on photoionization models with J. Krolik and W. Zheng. This work was supported by NASA contract NAS 5-27000 to the Johns Hopkins University.

REFERENCES

Antonucci, R. R. J., & Miller, J. S. 1985, ApJ, 297, 621
Armus, L., et al. 1991, BAAS, 23, 922
Avni, Y. 1976, ApJ, 210, 642
Blair, W. P., Long, K. S., Vancura, O., & Holberg, J. B. 1991a, ApJ, 374, 202
Blair, W. P., et al. 1991b, ApJ, 379, L33
Caganoff, S., et al. 1991, ApJ, 377, L9
Davidson, A. F., et al. 1992, ApJ, 392, 264
Elvis, M., & Lawrence, A. 1988, ApJ, 331, 161
Evans, I. N., Ford, H. C., Kinney, A. L., Antonucci, R. R. J., Armus, L., & Caganoff, S. 1991, ApJ, 369, L27
Fitzpatrick, E., & Massa, D. 1988, ApJ, 328, 734
Gaskell, C. M. 1982, ApJ, 263, 79
Hartigan, P., Raymond, J., & Hartmann, L. 1987, ApJ, 316, 323
Hutchings, J. B., et al. 1991, ApJ, 377, L25
Keenan, F. P., & Aggarwal, K. M. 1987, ApJ, 319, 403
Kinney, A. L., Antonucci, R. R. J., Ward, M. J., Wilson, A. S., & Whittle, M. 1991, ApJ, 377, 100
Koski, A. T. 1978, ApJ, 223, 56
Koyama, K., Inoue, H., Takano, S., Tanaka, Y., Ohashi, T., & Matsuoka, M. 1989, PASJ, 41, 731
Krolik, J. 1992, private communication
Krolik, J. H., & Begelman, M. C. 1986, ApJ, 308, L55
Krolik, J. H., McKee, C. F., & Tarter, C. B. 1981, ApJ, 249, 422
Kurucz, R. L. 1991, in Stellar Atmospheres: Beyond Classical Models, ed. L. Crivellari, I. Hubeny, & D. G. Hummer (Dordrecht: Kluwer), in press
Lawrence, A., & Elvis, M. 1982, ApJ, 256, 410
Longo, R., Stalio, R., Polidan, R. S., & Rossi, L. 1989, ApJ, 339, 474
Malkan, M. A., & Oke, J. B. 1983, ApJ, 265, 92
Marshall, F. E. 1991, BAAS, 23, 958
Meaburn, J., & Pedlar, A. 1986, AA, 159, 336
Miller, J. S., Goodrich, R. W., & Matthews, W. G. 1991, ApJ, 378, 47 (MGM)
Neugebauer, G., et al. 1980, ApJ, 238, 502
Nussbaumer, H., & Storey, P. J. 1978, A&A, 64, 139
———. 1979, A&A, 71, L5
———. 1982, A&A, 109, 271
Pogge, R. 1988, ApJ, 328, 519
Rowan-Robinson, M., et al. 1992, Nature, 351, 719
Seaton, M. J. 1978, MNRAS, 185, 5P
———. 1979, MNRAS, 187, 73P
Shields, G. A., & Oke, J. B. 1975, ApJ, 197, 5
Shull, J. M., & Van Steenberg, M. 1982, ApJS, 48, 95
Snijders, M. A. J., Netzer, H., & Boksenberg, A. 1986, MNRAS, 222, 549
Thronson, H. A., et al. 1989, ApJ, 343, 158
Viegas-Aldrovandi, S. M., & Contini, M. 1989, ApJ, 339, 689
Wilkes, B. 1984, MNRAS, 207, 73